Wavelength conversion of chaotic message through gain modulation by injection-locked Fabry-Perot laser diode

Yanqing Ding (丁燕青), Anbang Wang (王安帮), Mingjiang Zhang (张明江), Hucheng He (贺虎成), Xiaochun Li (李晓春), and Yuncai Wang (王云才)*

Physics Department, College of Science, Taiyuan University of Technology, Taiyuan 030024, China

**E-mail: wangyc@tyut.edu.cn*

Received June 22, 2009

We propose a wavelength conversion scheme for chaotic optical communications (COC) based on a Fabry-Perot (FP) laser diode. The FP laser, as a wavelength converter, is injection-locked at one of longitudinal modes by an external continuous-wave (CW) light. The simulation results demonstrated that the chaos masked signal at wavelength λ_1, which corresponds to the other longitudinal mode of FP laser, can be converted to the injection-locked mode (wavelength λ_2) based on cross-gain modulation in a closed-loop COC link. A 1.2-GHz chaos masked sinusoidal signal is successfully decoded with signal-to-noise ratio (SNR) beyond 8 dB in 15-nm wavelength conversion range, and the effects of SNR on the signal frequency and conversion span are also investigated.

OCIS codes: 060.0060, 140.1540, 230.7405, 140.5960.

doi: 10.3788/COL20100804.0368.

Chaotic optical communication (COC), a hardware cryptography technique utilizing the chaos synchronization between a pair of parameter-matched lasers[1], has attracted considerable interest due to its potential applications in spread spectrum secure communications. Argyris *et al.* successfully demonstrated a 120-km point-to-point field experiment in Athens[2]. A great deal of research focused on the applications of the COC in real, more complex networks. Multimode synchronization[3], message broadcasting[4] and relaying[5], multi-channel[6] transmission, demultiplexing[7], and wavelength division multiplexing (WDM)[8,9] techniques were proposed or demonstrated one after the other.

However, compared with the non-chaotic, conventional optical communication, wavelength conversion technique is still a challenge in COC. To the former, various all-optical wavelength conversion methods, such as nonlinear optical gating based on fiber loop, cross-gain modulation (XGM), cross-phase modulation, four-wave mixing (FWM) techniques, have been proposed. But in COC, the only all-optical wavelength conversion scheme, to our knowledge, was proposed by Annovazzi-Lodi *et al.*[10] who demonstrated that the FWM technology in a semiconductor optical amplifier can be used to convert the chaos masked signal to different wavelengths. In this letter, an injection-locked Fabry-Perot (FP) laser is used as a wavelength converter for COC, which has been investigated for non-chaotic communication system[11,12]. The higher injection optical power and strict phase-match conditions are not needed in our scheme.

The schematic diagram of wavelength conversion utilizing multimode FP laser in a close-loop COC system is shown in Fig. 1. The transmitter laser (TL) is the distributed feedback (DFB) laser diode (LD) with optical feedback from an external reflector and emits chaotic carrier at the central wavelength λ_1 under appropriate feedback parameters. The structure of the receiver laser (RL) is the same as that of the TL except for its operating wavelength λ_2. The messages are buried into the chaotic carrier (λ_1) by current modulation onto TL, i.e., chaos-shift-keying (CSK) modulation. Between the TL and RL, an injection-locked FP laser followed by an optical band-pass filter is inserted as the wavelength converter. Wavelengths λ_1 and λ_2 correspond to two longitudinal modes of FP laser. This FP semiconductor laser can be injection-locked at wavelength λ_2 by a wavelength tunable laser or a single-mode laser (such as a DFB semiconductor laser). Once the FP laser is injection-locked at wavelength λ_2, the transmitted signal (message + carrier) at wavelength λ_1 is converted into the target wavelength λ_2 owing to the XGM effect. The filter, after the FP laser is used to reject the residual power contributions at wavelength λ_1, passes through the signal at wavelength λ_2. The wavelength-converted signal is divided into two beams by a coupler: one is injected into the RL to achieve chaos synchronization, and the other is the reference beam from which the message can be obtained by subtraction of the synchronized carrier.

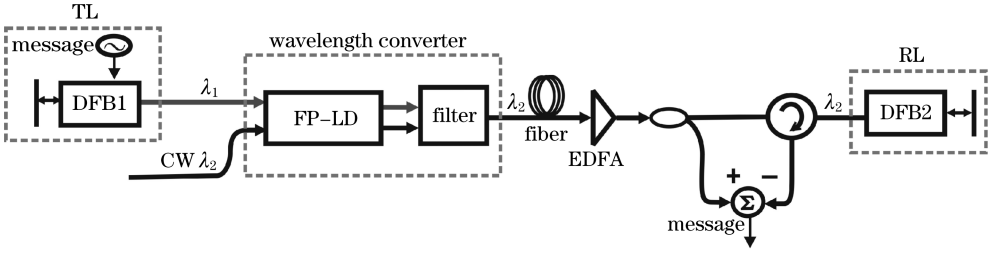

Fig. 1. Schematic of proposed wavelength conversion in COC system.

The dynamics of the TL and RL can be described by the modified Lang-Kobayashi rate equations with optical feedback and injection terms. For simplicity, we assume there are only two modes in the FP laser cavity. The rate equations of the FP laser are shown as

$$\frac{\mathrm{d}N(t)}{\mathrm{d}t} = \frac{I(t)}{qV} - \frac{N(t)}{\tau_\mathrm{n}} - \frac{S_1(t)[N(t)-N_0]g_1}{1+\varepsilon[S_1(t)+S_2(t)]} - \frac{S_2(t)[N(t)-N_0]g_2}{1+\varepsilon[S_1(t)+S_2(t)]}, \tag{1}$$

$$\frac{\mathrm{d}S_{1,2}(t)}{\mathrm{d}t} = \frac{\Gamma\beta N(t)}{\tau_\mathrm{n}} - \frac{S_{1,2}(t)}{\tau_\mathrm{P}} + \frac{S_{1,2}(t)[N(t)-N_0]g_{1,2}\Gamma}{1+\varepsilon[S_1(t)+S_2(t)]} + 2\frac{k_{\mathrm{inj}1,2}}{\tau_\mathrm{in}}\sqrt{S_{1,2}(t)P_{1,2}(t)}\cos\xi_{1,2}(t), \tag{2}$$

$$\frac{\mathrm{d}\varphi_{1,2}(t)}{\mathrm{d}t} = \frac{1}{2}\alpha g_{1,2}\Gamma\left\{\frac{N(t)-N_0}{1+\varepsilon[S_1(t)+S_2(t)]} - \frac{1}{\tau_\mathrm{P}}\right\} - \frac{k_{\mathrm{inj}1,2}}{\tau_\mathrm{in}}\sqrt{\frac{P_{1,2}(t)}{S_{1,2}(t)}}\sin\xi_{1,2}(t), \tag{3}$$

where subscripts 1 and 2 represent the different modes of λ_1 and λ_2 of the FP-LD, $S_{1,2}(t)$ and $\varphi_{1,2}(t)$ are the photon density and the phase of these two modes, respectively, $g_{1,2} = g_0/[1+(\lambda_{1,2}-\lambda_0)^2/\Delta\lambda^2]$ represent the gain coefficients at mode λ_1 and λ_2, $P_{1,2}(t)$ represent the injection photon densities from TL at wavelength λ_1 and injection light at wavelength λ_2, respectively, $N(t)$ is the carrier density; $I(t)$ is the bias current of the FP laser, and $\xi_{1,2}(t) = \varphi_{1,2}(t) + \Delta\omega t$, here $\Delta\omega$ is the frequency detuning between the injection light and the corresponding mode of the FP-LD ($\Delta\omega = 0$ in our simulation). The injection coefficient $k_{\mathrm{inj}1,2}$ from external optical injection to the FP-LD is defined as

$$k_{\mathrm{inj}1,2} = (1-r)\sqrt{(r_{\mathrm{inj}1,2}/r)}, \tag{4}$$

where r represents the amplitude reflectivity of the laser cavity facet, and $r = 0.3$ since the cavity facets are as-cleaved. The injection strength $r_{\mathrm{inj}1,2}$ represents the percentage ratio of the external optical power injected into the laser cavity to the laser output power, $r_{\mathrm{inj}1,2} = 50\%$. To realize chaos synchronization between the FP-LD and the RL, we set the main parameters of these two semiconductor lasers equal. The typical values for all the internal parameters in our numerical simulation are listed in Table 1.

In this letter, our main purpose is to study whether an injection-locked FP laser can be used as a wavelength converter in COC, so a sinusoidal signal is used as the chaos-masked signal in our proof-of-concept scheme. The message is embedded in chaotic carrier by CSK modulation. Thus the driven current of the TL can be written as $I = I_\mathrm{b} + m(I_\mathrm{b} - I_\mathrm{th})\sin(2\pi ft)$, where I_b is the bias current of the TL, f is the frequency of message, and m is the modulation depth.

We first investigated the optical spectrum of the injection-locked FP laser. Figure 2(a) shows the optical spectrum of the two longitudinal modes FP laser under free-running at $I_\mathrm{b} = 30.14$ mA ($2.2I_\mathrm{th}$). The optical power at λ_1= 1554.8 nm is less than that at λ_2= 1550 nm since λ_1 is near 5 nm far away from the central wavelength. When the wavelength of external injection light is close to wavelength λ_2, FP laser is injection-locked and λ_1 mode is suppressed. Figure 2(b) shows the corresponding optical spectrum when the FP laser is injection-locked at wavelength λ_2 by an external optical source. When the injection-locked FP laser is inserted into the closed-loop COC link, the optical power of λ_2 mode is modulated by the signal power of wavelength λ_1 because of the XGM effect in the FP laser cavity, and the message in the λ_1 mode is converted into the λ_2 mode, i.e., from 1554.8 to 1550 nm. Figure 2(c) shows the optical spectrum of the injection-locked FP laser under chaotic carrier injection. It is obvious that the optical power of λ_1 mode is amplified because the FP laser is dual-mode injection locked in this case. Especially, we find that the spectra of both modes are broadened after being injected, which indicates that both modes operate into chaotic oscillation state, and λ_2 mode is modulated by λ_1 mode based on XGM effect.

The TL can emit chaotic light when its feedback coefficient k_T is 0.003 at bias current I_b of 20.55 mA ($1.5I_\mathrm{th}$).

Table 1. Parameter Values of the Semiconductor Lasers Used in Simulations

Symbol	Parameter	Value
q	Electron Charge	1.602×10^{-19} C
V	Active Region Volume	1.2×10^{-16} m^3
τ_n	Carrier Lifetime	2 ns
τ_p	Photon Lifetime	2 ps
τ_in	Round-trip Time in the Internal Laser Cavity	10 ps
Γ	Optical Confinement Factor	0.5
N_0	Carrier Density at Transparency	10^{24} m^{-3}
N_th	Carrier Density at Threshold	1.5×10^{24} m^{-3}
I_th	Threshold Current	13.7 mA
α	Linewidth Enhancement Factor	3
λ_0	Center Wavelength	1550 nm
g_0	Gain Coefficient of the Central Wavelength	2×10^{-12} m^3/s

Figure 3(a) shows the time traces of the TL. When the injection-locked (at λ_2) FP laser is injected by chaotic carrier at wavelength λ_1, the output power of wavelength λ_2 will be modulated by the intensity fluctuation of wavelength λ_1. The output time traces of the wavelength converter will synchronize reversedly with the injection chaotic carrier. Figure 3(b) shows clearly the anti-phase synchronization between the two modes of the FP laser. Figure 3(c) shows the cross-correlation traces of the two modes, the corresponding correlation coefficient is –0.87.

The output of the receiver will synchronize with the injection chaotic carrier under appropriate condition. By adjusting the injection strength and feedback coefficient (here the injection strength $r_{\mathrm{injR}} = 50\%$ and k_{R}= 0.003), we can obtain 0.96 correlation coefficient between the converted chaotic carrier and the RL output. A 0.5-GHz sinusoidal signal with modulation depth of 0.5 is used as the message signal, which is encoded by CSK modulation. Figures 4(a), (c), and (e) are the time series of the output of the TL, wavelength converter and RL,

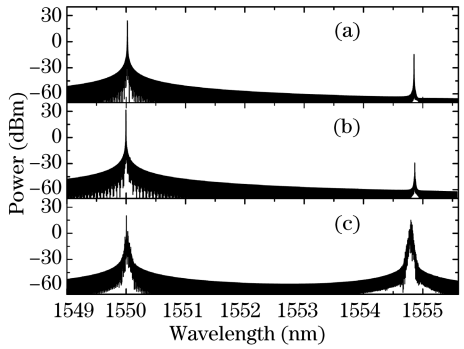

Fig. 2. Output optical spectra of the FP-LD (a) without injection, (b) injection-locked, and (c) with injection.

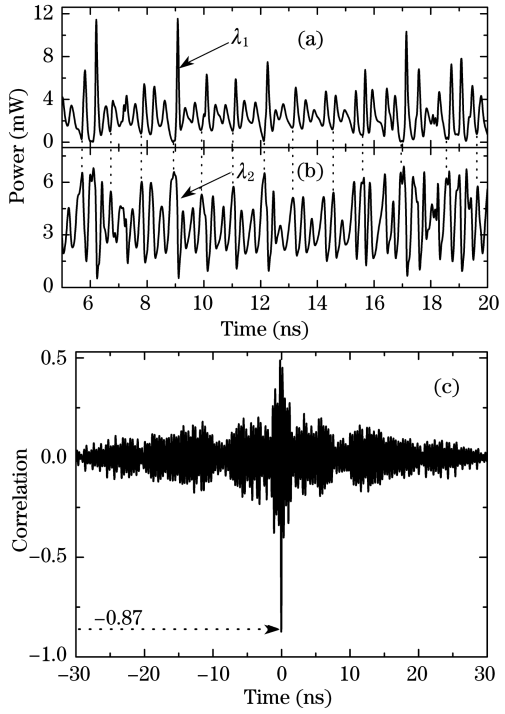

Fig. 3. Time traces of (a) TL, (b) filtered FP-LD, and (c) relationship between them when there is no encoded message.

respectively. Their corresponding power spectra are listed on the right column of Fig. 4. The message signal component (shown by the arrows) is clearly seen in Figs. 4(b) and (d), but not pronounced in Fig. 4(f) because of the filtering characteristics of the RL. Figures 4(g) and (h) show the extracted message signal by subtracting the waveform in Fig. 4(e) from that in Fig. 4(c), and the corresponding power spectrum, respectively. Figure 4(h) indicates that the receiver retrieves the transmitted message with signal-to-noise ratio (SNR) up to 20 dB. Figures 4(g) and (h) demonstrate that our method is successful for wavelength conversion in COC.

We also simulated the SNR of the recovered signal at different longitudinal modes. Figure 5 exhibits the calculated SNRs of 0.5- and 1.2-GHz transmitted signal at different wavelength conversion span ($\Delta\lambda = \lambda_1 - \lambda_2$, λ_1 and λ_2 are the integer of 0.8-nm FP laser longitudinal mode separation). Figure 5 indicates that the SNR decreases with the increase of the signal frequency. For the TL used, the SNR of recovered signal maintained beyond 8 dB in 15-nm wavelength conversion range although its free-running relaxation oscillation frequency was only 2.7 GHz at 20.55-mA bias current ($I_{\mathrm{b}} = 1.5I_{\mathrm{th}}$); the larger SNR is obtained when $\Delta\lambda \geq \pm 4$ nm, and when $\Delta\lambda > 0$ the SNR is larger than that of $\Delta\lambda < 0$. These phenomena are similar to the relationship of the extinction ratio of wavelength converted signal to the wavelength conversion span[13]. The maximum SNR is 22.4 dB while the wavelength spacing value is 5.6 nm for the message of 0.5 GHz. The main disadvantage of our method is that the wavelength conversion can only be implemented discretely, corresponding to the mode separation of FP laser. Fortunately, we can tune the wavelength by changing the operating temperature of the lasers. In particular, the wavelength of channels is normally fixed in WDM communication systems.

The filtering effect of RL at different signal frequencies is shown in Fig. 6. The SNR decreases as the message frequency increases, and drops down to 3 dB when the signal frequency approaches to the TL's relaxation frequency of 2.7 GHz. Although the SNR deteriorates about 10 dB when an injection-locked FP laser is inserted into COC system as a wavelength converter, the upper limit of transmission rate, which is determined by the

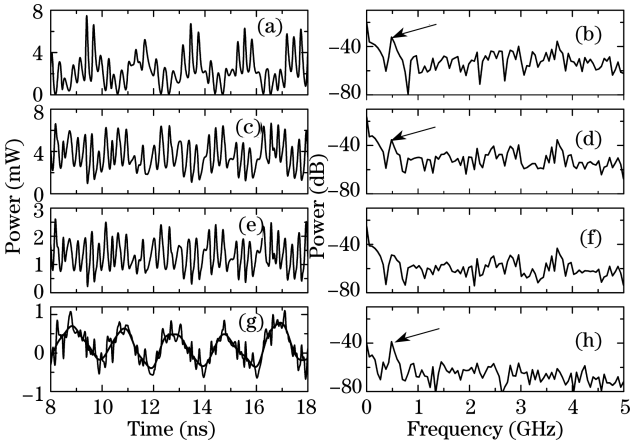

Fig. 4. Time traces of (a) output of the TL, (c) wavelength converter, (e) RL, and (g) extracted signal. (b), (d), (f), and (h) are power spectra corresponding to (a), (c), (e), and (g).

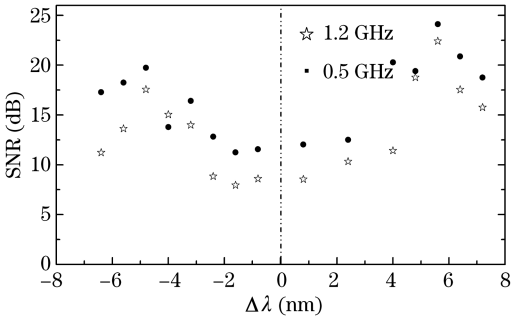

Fig. 5. SNR as a function of the wavelength conversion span.

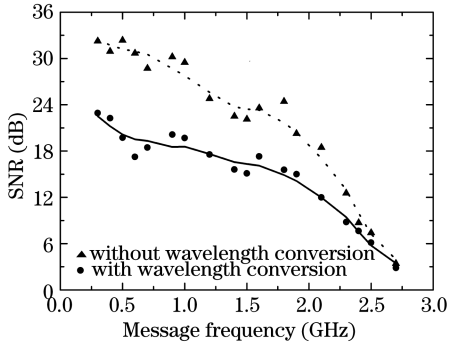

Fig. 6. SNR as a function of the message frequency.

relaxation oscillation frequency of RL[14,15], is not limited by the wavelength converter. This indicates that our method can be used in high speed COC system.

In conclusion, we present and numerically demonstrate the wavelength conversion for COC by utilizing the injection-locked FP laser as the wavelength converter. 1.2-GHz sinusoidal signal is successfully decoded with the SNR beyond 8 dB in 15-nm wavelength conversion range. Meanwhile, the obtained results indicate that this method does not affect the transmission rate.

This work was supported by the National Natural Science Foundation of China (No. 60777041) and the International Cooperation Fund of Shanxi Province of China (No. 2007081019).

References

1. G. D. Van Wiggeren and R. Roy, Science **279,** 1198 (1998).
2. A. Argyris, D. Syvridis, L. Larger, V. Annovazzi-Lodi, P. Colet, I. Fischer, J. García-Ojalvo, C. R. Mirasso, L. Pesquera, and K. A. Shore, Nature **438,** 343 (2005).
3. M. W. Lee and K. A. Shore, J. Lightwave Technol. **23,** 1068 (2005).
4. M. W. Lee and K. A. Shore, Electron. Lett. **40,** 614 (2004).
5. M. W. Lee and K. A. Shore, IEEE Photon. Technol. Lett. **18,** 169 (2006).
6. J. Paul, S. Sivaprakasam, and K. A. Shore, J. Opt. Soc. Am. B **21,** 514 (2004).
7. J. M. Buldú, J. García-Ojalvo, and M. C. Torrent, IEEE J. Quantum Electron. **41,** 164 (2005).
8. T. Matsuura, A. Uchida, and S. Yoshimori, Opt. Lett. **29,** 2731 (2004).
9. J.-Z. Zhang, A.-B. Wang, J.-F. Wang, and Y.-C. Wang, Opt. Express **17,** 6357 (2009).
10. V. Annovazzi-Lodi, G. Aromataris, M. Benedetti, I. Cristiani, S. Merlo, and P. Minzioni, IEEE Photon. Technol. Lett. **19,** 1783 (2007).
11. H. K. Tsang, L. Y. Chan, S. P. Yam, and C. Shu, Opt. Commun. **156,** 321 (1998).
12. H. Jiang, K. Wu, L. Han, X. Teng, and H. Zhang, Chinese J. Lasers (in Chinese) **32,** 1183 (2005).
13. Y. An, Y. Wang, M. Zhang, S. Niu, and A. Wang, Acta Phys. Sin. (in Chinese) **57,** 4995 (2008).
14. A. Uchida, Y. Liu, and P. Davis, IEEE J. Quantum Electron. **39,** 963 (2003).
15. J. Paul, M. W. Lee, and K. A. Shore, Opt. Lett. **29,** 2497 (2004).